Molecular Crystals and Liquid Crystals Science and Technology. Section A. Molecular Crystals and Liquid Crystals

Publication details, including instructions for authors and subscription information:
http://www.tandfonline.com/loi/gmcl19

Electron and Hole Mobilities in High Purity Anthracene Single Crystals

Norbert Karl [a] & Jörg Marktanner [a b]

[a] 3. Phys., Inst. Univ. Stuttgart, D-70550, Stuttgart, Germany

[b] TRIKON Technologies GmbH, Herrlinger Str. 36, D-89081, Ulm

Version of record first published: 24 Sep 2006

To cite this article: Norbert Karl & Jörg Marktanner (2001): Electron and Hole Mobilities in High Purity Anthracene Single Crystals, Molecular Crystals and Liquid Crystals Science and Technology. Section A. Molecular Crystals and Liquid Crystals, 355:1, 149-173

To link to this article: http://dx.doi.org/10.1080/10587250108023659

Mol. Cryst. Liq. Cryst., Vol. 355, pp. 149-173
Reprints available directly from the publisher
Photocopying permitted by license only

Electron and Hole Mobilities in High Purity Anthracene Single Crystals*

NORBERT KARL† and JÖRG MARKTANNER‡

3. Phys. Inst. Univ. Stuttgart, D-70550 Stuttgart, Germany

(Received December 31, 1999; In final form February 03, 2000)

Using ultrapurified, highly perfect anthracene crystals electron and hole mobility data were measured by the time-of-flight method over a wide temperature range along 5 different crystallographic directions. From these results full tensor data (principal axes mobilities, tensor orientations and tensor rotations with temperature) have been determined. The highest principal electron mobility component is close to the *a* axis, reaching 35cm^2/Vs at 20K, the highest hole component along *b*, reaching 50cm^2/Vs at 35K. For electrons moving along the crystallographic *c'* direction a transition from a nearly temperature-independent mobility (400K- 100K) to a mobility increasing upon further cooling has been found, with very similar absolute values and transition temperature as previously reported for naphthalene and explained as a hopping to band transition. A non-Ohmic, sublinear velocity – electric field relation, reflecting hot charge carriers, has been obtained between 20 and 36K for electrons drifting along *a*, with a tendency of velocity saturation between 0.5 and 1·10^{6}cm/s, similar to what has been reported before for naphthalene and perylene. Different samples set different low temperature limits to a determination of microscopic time-of-flight mobilities by an onset of trapping, probably at structural defects, induced during handling and measurement.

Keywords: anthracene; photoconduction; mobilities; nonlinear transport

INTRODUCTION

Forty years ago Kepler [1] and LeBlanc [2] independently reported electron and hole mobilities in single crystals of the organic photoconductor anthracene, measured by the time of flight (TOF) method. This was a landmark in two respects:

(1) These authors were the first to introduce this very direct method to the field of organic materials.

* ....dedicated to a friend

† Corresponding Author: e -mail: n.karl@physik.uni-stuttgart.de

‡ Present address: TRIKON Technologies GmbH, Herrlinger Str. 36, D-89081 Ulm.

(2) Using well purified material, they found reliable microscopic mobilities, essentially uninfluenced by multiple shallow trapping retardation.

The TOF method is a rather direct measurement technique for determining mobilities of charge carriers in that it directly visualizes their transit motion through a crystal slice (sandwiched between and capacitively coupled to two electrodes), from the start near the flash-illuminated electrode to the arrival at the opposite one.

While Kepler observed the carrier motion via the short circuit current $j(t)$ in the external circuit (of a sufficiently low RC time constant) as $U(t) = R \cdot j(t)$, LeBlanc used the integrating method, based on an RC product large against typical transit times, which yields $U(t) = \frac{1}{C}\int_0^t j(t)dt$.

The anthracene mobility data available from different authors until ca. 1984 [1–3] have been summarized in a data compilation [4]. We subsequently took great efforts to still improve crystal purity and perfection, which allowed us to make considerable progress in four directions:

(1) To measure mobilities at much lower temperatures and to so obtain much higher values than previously reported for the higher temperatures, confirming a negative mobility/temperature gradient for the pure crystal.

(2) To detect also in anthracene the existence of an anomalous temperature dependence for the electron motion in the weak coupling crystallographic c' direction, an effect previously only known for naphthalene [5–7], which had heated up considerable debates on the underlying transport mechanisms, culminating in the statement that it reflected a transition from an incoherent hopping to a coherent band type transport regime upon cooling, unique for this crystallographic direction and charge carrier sign [5,6].

(3) To discover nonlinear (i. e. non-Ohmic) transport at low temperatures, similar to what we had found for naphthalene [8] and perylene [9], and later for biphenyl [10].

(4) To determine full anisotropic mobility tensor data across a considerable temperature range.

Summarizing these results briefly already here, one can note down: In a sufficiently pure and crystallographically perfect anthracene crystal electron and hole mobilities μ increase continuously upon cooling, following a $\mu \propto T^n, -3 < n < -1$ temperature dependence, very similar to typical inorganic semiconductors where such a temperature dependence is explained by scattering at occupied acoustical/optical phonon modes. Even the electron mobility in c' direction which appears almost temperature-independent over a wide temperatur range (400–80K), finally starts to increase upon further cooling below 80K.Thus in a suffi-

ciently pure and perfect anthracene crystal neither the fundamental transport property of the electron nor that of the hole is thermally activated at low temperature. Moreover, the velocity – field relation in the low temperature high mobility regime is nonlinear (i.e. transport is non-Ohmic), with tendency towards velocity saturation for high field strength, which can be explained on the basis of warm ("hot") electrons, heated by the field acceleration, which loose energy by collisions with the crystal lattice under generation of phonons, i.e. by "generative phonon scattering", cf. [8].

In what follows, we wish to present an ample set of temperature-dependent full tensor data of electron and hole mobilities in anthracene and to discuss various interpretational aspects in some detail.

EXPERIMENTAL

The time-of-flight method

The principle and several experimental details of the time-of-flight, TOF, method for determining charge carrier mobilities in photoconductors have already been communicated elsewhere [8,9,11–17]. It may thus suffice to summarize: Charge carrier pairs are created in a photoconductor, near the surface of a plane-parallel crystal slice sandwiched between two planar electrodes, by absorption of a short pulse of light of sufficient photon energy, admitted through the semitransparent front electrode. Depending on the polarity of the field E established by applying a voltage difference between the front and a rear electrode (separated by a distance L) a "sheet" of electrons or holes is pulled across the crystal at a velocity $v = \mu E$. In the external circuit a constant current flows, coupled by the displacement current, which drops to 50% (or to zero) when 50% (or all) moving carriers have been collected by (or stopped near) the rear electrode. The average travel time τ, read from the duration of an (ideally) rectangular TOF pulse on an oscilloscope display, is thus a direct measure of the (average) drift velocity v of the carriers, $v = L/\tau$. This statement needs further explanations: The drift current is only constant before the first carriers arrive, if the number of mobile charge carriers underway is not reduced by trapping losses and if the transported (extra) charge is small enough to not disturb the applied field, and thus travels at constant velocity. For a strongly absorbed excitation light pulse of duration $\delta t \ll \tau$, and fast carrier generation, the starting charge carrier sheet has a width $\delta \ell \ll L$. This width is slightly increased during travel by diffusion and Coulombic repulsion broadening, cf. [12], but it usually remains narrow against L, thus defining a

rather narrow arrival time distribution and a rather sharp average of the arrival times. A typical near ideal electron drift current pulse is displayed in Fig. 1a. If trapping losses are not so severe as to preclude the detection of arriving charge carriers, mobility can even be determined in presence of a certain (small) amount of (trap forming) impurities, see Fig. 1b; in such situations obviously a shorter interaction time (and hence transit time) at a higher field or in a thinner sampler will be beneficial. Needless to say that if no clear arrival time kink is seen in the transit pulse, extraction of velocity and mobility data is impossible and such results should be disregarded. It should also be mentioned that occasionally even for well ordered crystals dispersive transport (see eg. [18]) has been observed *at very low temperatures* (probably caused by lattice defects and strain, leading to a wide energetic distribution of shallow traps; an example can be found in Fig. 1.17 of ref. [17]). Dispersive transport does not allow to assign a material property "mobility" to a sample, because in dispersive transport there is a wide distribution of arrival times and the velocity of each charge carrier drops with time going on, i.e. there are no reasonable average values characteristic of the material as such.

Sample preparation

Synthetic (i.e. not from coal tar extracted) anthracene (Eastman Kodak) was vacuum-sublimed at 190°C and then subjected to a sequence of zone refining steps in three different zone refining tubes, combining vertical and horizontal zone refining techniques, and using only the purest fractions of a previous zone-refined ingot distinguished by a triplet exciton lifetime $\tau_{Tr} \geq 20$ms for filling the next one (cf. ref. [19]). All together 600 passages of molten zones at $L/\ell \approx 25$ (cf. ref. [19]) were applied. From a final polycrystalline fraction with $\tau_{Tr} = 25$ms a single crystal of 15mm Ø was grown by slow directional cooling (Bridgman method, cf. [19]) which displayed $\tau_{Tr} = 19$ms immediately after growth. It should be mentioned that the crystal used in the measurements to be presented here had then several years time to anneal in the evacuated growth ampoule (at room temperature).

Slices were cut in different crystallographic orientations by cautious dissolution sawing on a thread saw, using a thin polyester thread, xylene as a solvent, and very small press-on force. By a suitable choice of the latter and of the solvent drop rate to the thread a rather smooth surface could be obtained ($\Delta L < \pm 20\mu$m for $L = 300\mu$m); as anthracene is rather soft and displays a pronounced propensity towards gliding no further polishing was applied to avoid introduction of defects. Thickness of individual samples was measured (after the electrical measurements were finished) by a dial gauge and rechecked, after cutting with a razor blade, under a measurement microscope, for control of thickness, parallelism and roughness.

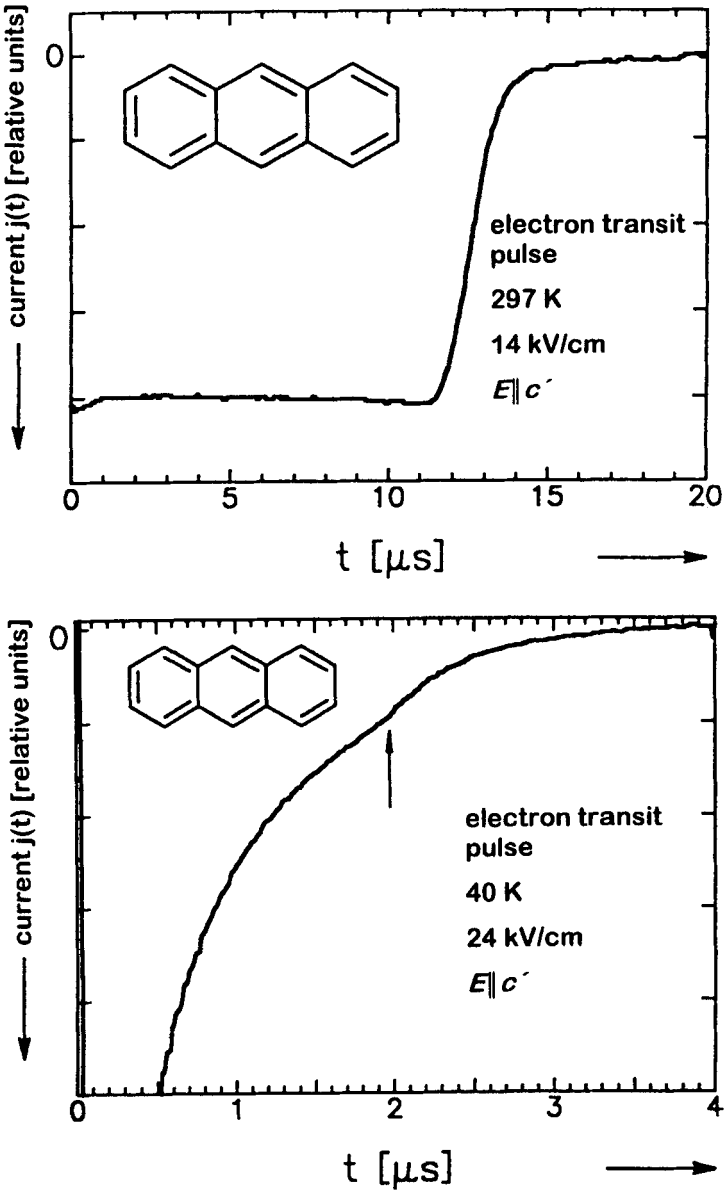

FIGURE 1 (a) Near ideal electron TOF drift current pulse (negative amplitude) across an anthracene crystal slice at 297K and a field of 14kV/cm along c'. No trapping influences are seen. (b) At 40K trap release times become much longer. As a consequence of trapping the TOF drift current pulse displays a strong exponential decay and only a small fraction of charge carriers arrive at the rear electrode, causing even at an increased field of 24kV/cm only a barely discernible indication of an arrival time kink (marked by an arrow)

Sample orientation and tensor presentation

The precise crystallographic orientation of each sample was determined, after completion of the electrical measurements, by comparison of experimental Laue X-ray diffraction patterns with calculated ones, cf. [20]. The orientations of all samples used are given in Table I and presented in stereographic projection in Fig. 2. Notice that from the monoclinic symmetry of the anthracene crystal structure the mobility tensors should be anisotropic with three different principal axes mobilities which can vary independently with temperature. One principal axis $\mu_{bb} = \mu_{22}$ of the mobility tensor (a symmetric polar material tensor of the second rank) is fixed by the twofold screw axis rotation symmetry of the anthracene structure along the crystallographic b axis, whereas the orientations of the other two principal axes are not determined by any symmetry constraints and hence a priory unknown (cf. ref. [4], p. 110).

TABLE I Orientations of the normals of the measured anthracene slices relative to the (orthogonalized) crystallographic axes a, b, and c', (c' | a×b ∥ c*), and symbols assigned to these orientations in the figures and in the text; cf. Fig. 2

No	*angle to*			*labelled in the text as*
	a	*b*	*c'*	
1	8.0	85.8	83.2	a
2	85.5	6.5	85.3	b
3	91.0	93.0	3.2	c'
4	123.5	90.0	33.5	S1
5	156.5	95.0	67.1	S2

Electrical measurements

The electrical rear contact of the crystal sample and thermal contact to a 15mm Ø copper support disc was either made by silver paint or by a liquid (eutectic) alloy of indium and gallium, also used for all other thermal contacts. The copper disc rested on an electrically insulating disc of BeO, which is a good thermal conductor, the latter on the cold finger of a helium flow cryostat. The front contact was usually a vacuum vapor-deposited semitransparent silver film of between 25 and 100 mm^2 area adapted to the sample size.

Depending on the required time resolution, a low noise cathode follower or a (faster) FET probe were used to pick up signals across an electrical vacuum feed-through as close as possible to the sample. Compromises between the optimal pick-up time constant and the short circuit current sensitivity were made by using appropriately chosen parallel input resistors. TOF signals were displayed single shot on a fast oscilloscope, the transient screen image picked up by a CCD camera and digitized as $j(t)$ files on a PC; more details may be found in ref. [15].

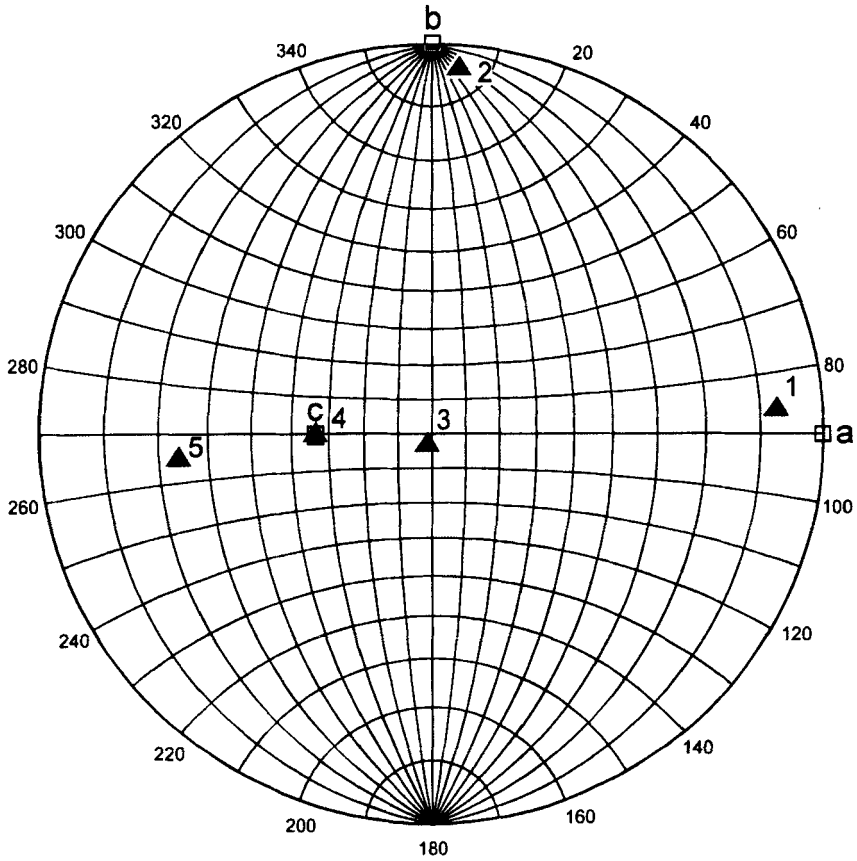

FIGURE 2 Presentation of the directions of the normals to the used crystal slices (which, at the same time, are the directions of the applied field) in stereographic projection. The crystallographic axes *a, b, c*, are marked by squares. The orientations 1, 3, 4, 5 were selected essentially perpendicularly to *b*, which is a principal axis direction, to arrive at a good determination of the rotation angle α of the larger principal mobility component in the *ac* plane relative to *a* (from where α is counted in the same sense as the monoclinic angle $\beta = 125°$), cf. Fig. 12

RESULTS AND DISCUSSION

Primary results

Electron and hole mobilities as a function of temperature are presented in log μ versus logT plots in Fig. 3, 4, and 5 for the electric field approximately (see Table I) along the crystallographic *a, b*, and *c'* direction, respectively; the results

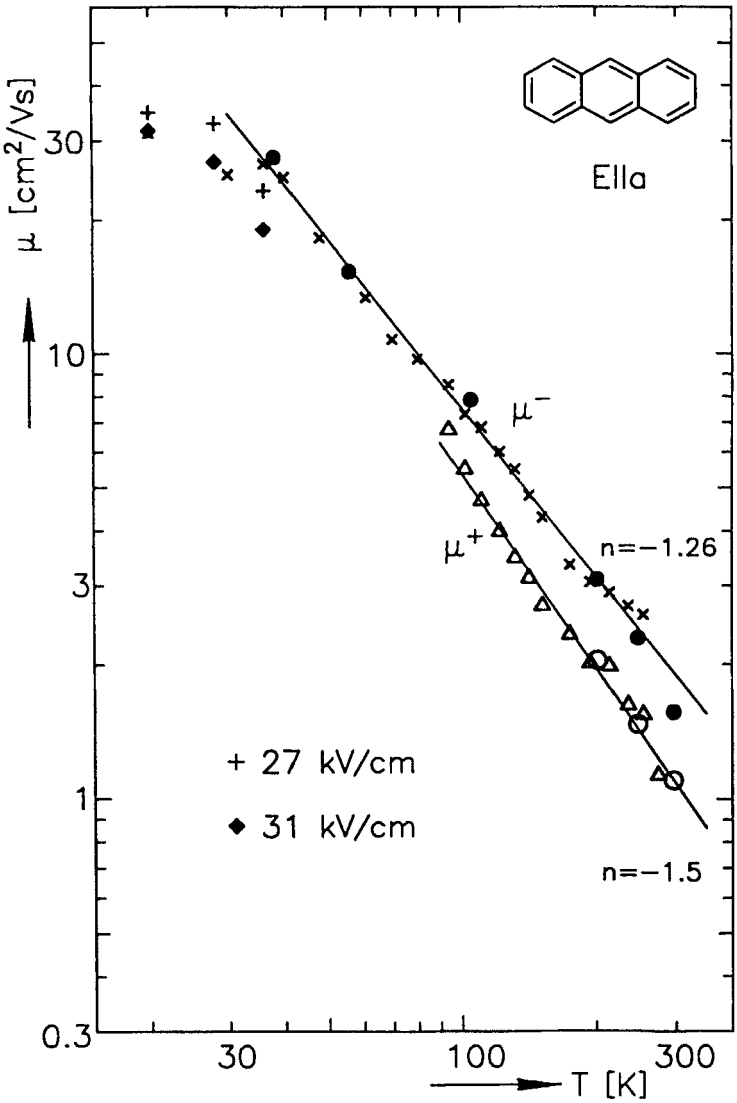

FIGURE 3 Electron and hole mobilities in the direction "1" ($\approx a$, cf. Table I), log μ versus log T plot. The different symbols mark two subsequent measurement cycles upon cooling. At low temperature/high mobility the mobilities apparently decrease with increasing electric field strength. Highest measured electron mobilities are around $30 cm^2/Vs$

obtained in the directions S1 and S2 (cf. Table I) are displayed in the Fig. 6 and 7, respectively. Except fot the 300 – 80K part of μ_c^-, all $\mu_{ij}(T)$ values increase with decreasing temperature, following a power law $\mu \propto T^n$temperature depend-

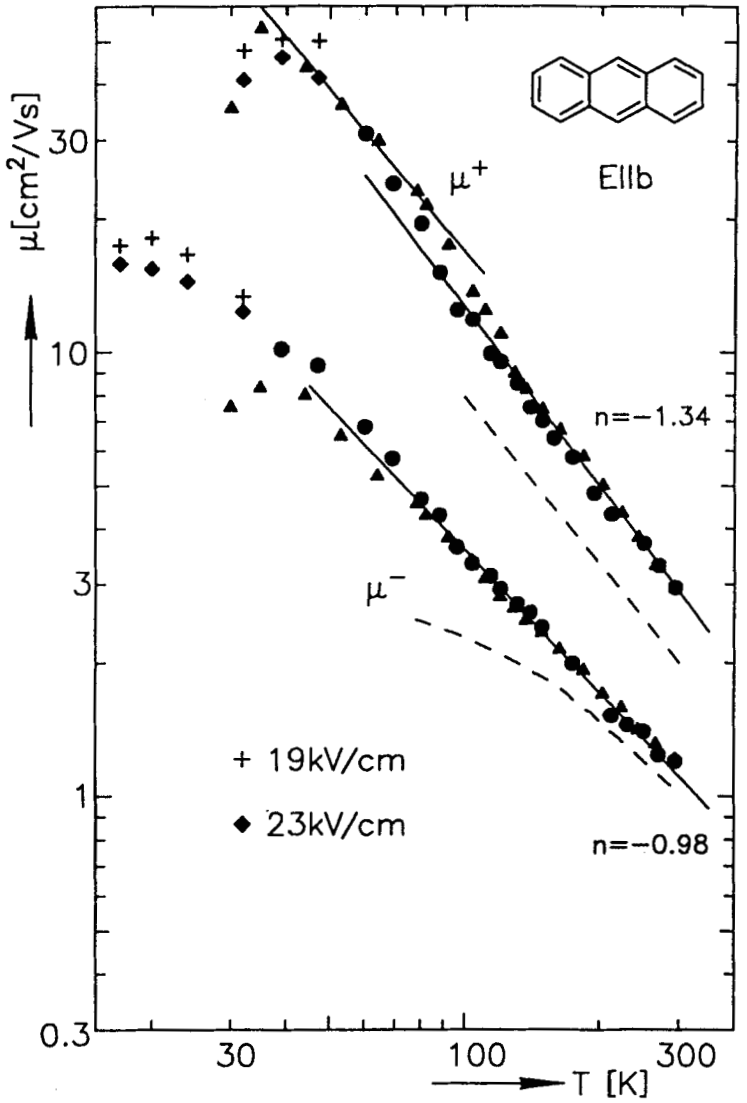

FIGURE 4 Electron and hole mobilities in the direction "2" (≈ *b*, cf. Table I), log μ versus log T plot. The different symbols mark two subsequent measurement cycles upon cooling. At low temperature/high mobility the mobilities apparently decrease with increasing electric field strength. Highest measured hole mobilities are around 50cm^2/Vs. Below 35K marked trapping influences become noticeable. The dashed lines indicate previously reported data [4,7] for comparison

ence with n generally different for electrons and holes, smaller for the electrons, and rather anisotropic, $-2.4 < n \leq -1$. The highest measured mobility values were

$30 cm^2/Vs$ for electrons in *a* direction, and 50 cm^2/Vs for holes in *b* direction. Comparison with earlier TOF results, cf. [4, 7], which did not reach below 80K because of trapping problems, shows that the purer and crystallographically more perfect crystal used in the present investigation not only allowed us to obtain microscopic mobility data at much lower temperature, but also generally led to slightly steeper slopes of the mobility curves in the logμ versus log$T$ presentations, and to somewhat larger mobility values, especially at the lower temperature bound of the earlier results. Both effects can essentially be attributed to a smaller concentration of shallow traps, whose presence leads to multiple shallow trapping-reduced "effective" mobilities, cf. the theoretical curves presented in ref. [16]. For a comparison of the present results with earlier ones, see [39].

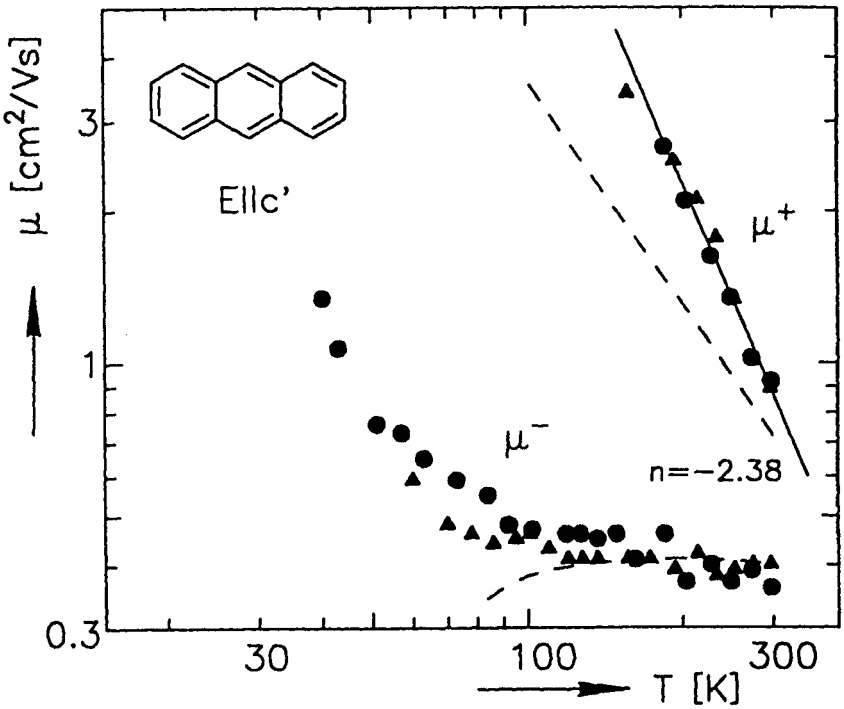

FIGURE 5 Electron and hole mobilities in the direction "3" ($\approx c'$, cf. Table I), log μ versus log T plot. The different symbols mark two subsequent measurement cycles upon cooling. The dashed lines indicate previously reported data [4, 7]

The mobility values plotted in these figures are based on the actually measured flight times, and therefore defined as the velocity component parallel to the field direction per unit field, the so- called "mobilities parallel to the given direction of

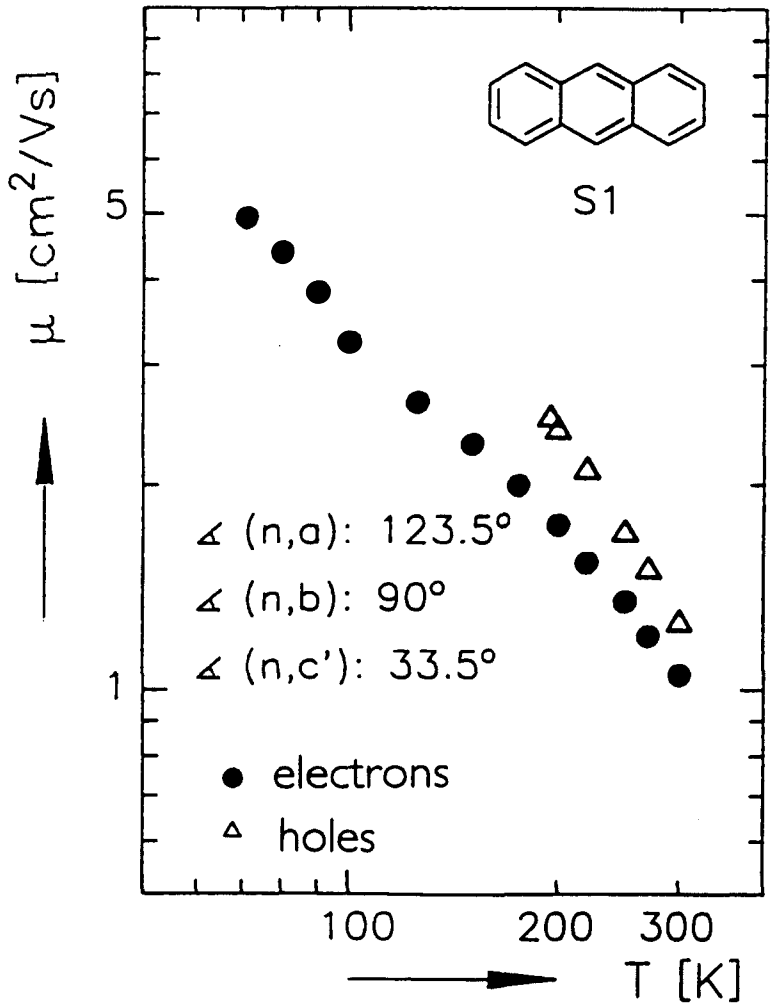

FIGURE 6 Electron and hole mobilities in the "S1"-direction (cf. Table I), log μ versus log T plot; averaged values of three runs. The mobilities of the holes follow a temperature dependence $\mu^+ \propto T^{-1.6}$, those of the electrons $\mu^- \propto T^{-1.0}$

the field" (cf. ref. [4], p. 110), $\mu_\parallel = \nu_\parallel / |E|$, whereas the true direction of motion is not in general parallel to the field vector, but more or less oblique to it, as a consequence of the tensorial relation $\nu_i = \mu_{ij} E_j$. Notice that e.g. for the direction a of the normal to the crystal slice, i.e. with the applied field $E = (E_a\ 0\ 0)$ the measured velocity component in the field direction is ν_a, hence the obtained tensor componente is $\mu_{aa} = \nu_a / E_a$, but there are, in general, also (small) orthogonal com-

ponents, e.g. $v_c = \mu_{ca} E_a$ which are not measured in the TOF experiment considered. The task to be solved now is to construct a best tensor (ellipsoid) from the five primary mobility values obtained for the five chosen directions at every measurement temperature, for the electrons as well as for the holes.

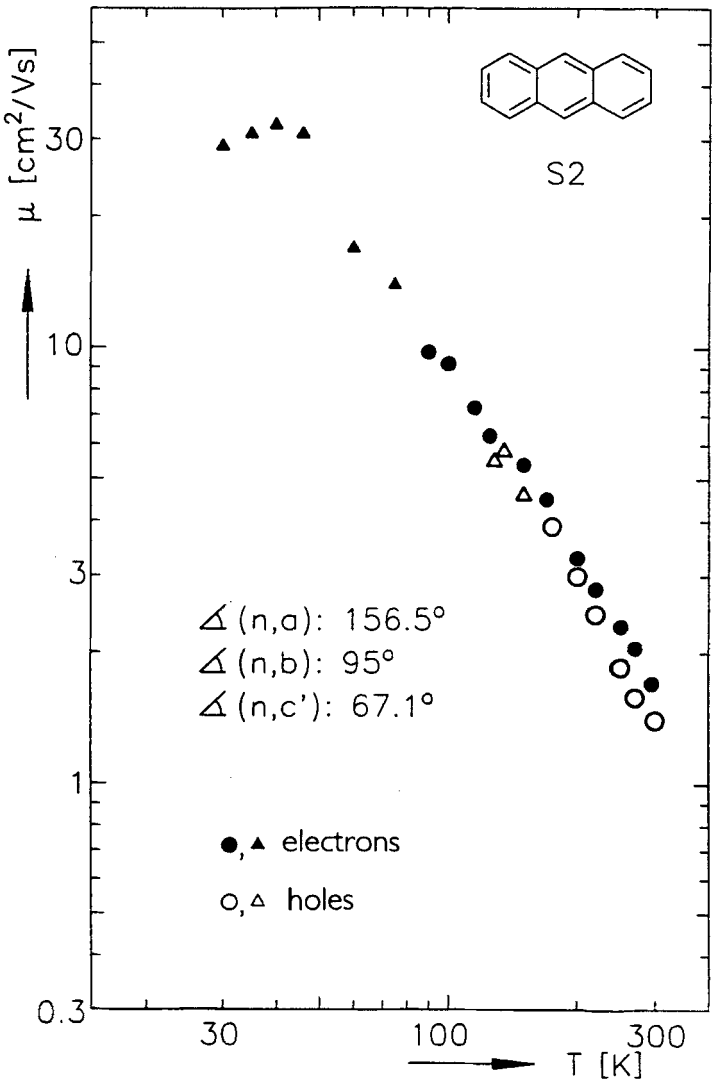

FIGURE 7 Electron and hole mobilities in the "S2"-direction (cf. Table I), log μ versus log T plot; (●, O) averaged values of three runs, (Δ, ▲) one run only. Notice that in this direction electrons and holes have nearly the same mobilities. The mobilities of the holes follow a temperature dependence $\mu^+ \propto T^{-1.8}$, those of the electrons $\mu^- \propto T^{-1.6}$

TABLE II The tensor of the hole mobility in anthracene in the orthogonalized crystallographic coordinate system *a, b, c'* at different temperatures (mobilities are in cm^2/Vs)

$$\underline{\underline{\mu}} = \begin{pmatrix} \mu_{aa} & \mu_{ab} & \mu_{ac'} \\ \mu_{ba} & \mu_{bb} & \mu_{bc'} \\ \mu_{c'a} & \mu_{c'b} & \mu_{c'c'} \end{pmatrix}$$

$$\underline{\underline{\mu}}^{+}(300K) = \begin{pmatrix} 1.140 & 0 & -0.366 \\ 0 & 2.930 & 0 \\ -0.366 & 0 & 0.846 \end{pmatrix}$$

$$\underline{\underline{\mu}}^{+}(250K) = \begin{pmatrix} 1.513 & 0 & -0.469 \\ 0 & 3.738 & 0 \\ -0.469 & 0 & 1.199 \end{pmatrix}$$

$$\underline{\underline{\mu}}^{+}(200K) = \begin{pmatrix} 2.221 & 0 & -0.611 \\ 0 & 5.052 & 0 \\ -0.611 & 0 & 1.981 \end{pmatrix}$$

TABLE III The tensor of the electron mobility in anthracene in the orthogonalized crystallographic coordinate system *a, b, c'* at different temperatures (mobilities are in cm^2/Vs)

$$\underline{\underline{\mu}}^{-}(300K) = \begin{pmatrix} 1.683 & 0 & -0.324 \\ 0 & 1.156 & 0 \\ -0.324 & 0 & 0.384 \end{pmatrix}$$

$$\underline{\underline{\mu}}^{-}(250K) = \begin{pmatrix} 2.285 & 0 & -0.378 \\ 0 & 1.386 & 0 \\ -0.378 & 0 & 0.383 \end{pmatrix}$$

$$\underline{\underline{\mu}}^{-}(200K) = \begin{pmatrix} 3.231 & 0 & -0.571 \\ 0 & 1.737 & 0 \\ -0.571 & 0 & 0.385 \end{pmatrix}$$

$$\underline{\underline{\mu}}^{-}(150K) = \begin{pmatrix} 4.967 & 0 & -0.671 \\ 0 & 2.356 & 0 \\ -0.671 & 0 & 0.388 \end{pmatrix}$$

$$\underline{\underline{\mu}}^{-}(110K) = \begin{pmatrix} 7.395 & 0 & -0.762 \\ 0 & 3.254 & 0 \\ -0.762 & 0 & 0.412 \end{pmatrix}$$

Determination of the best mobility tensors at the different temperatures

For presenting full mobility tensor data for a monoclinic crystal it is necessary to evaluate at least 4 independent mobility measurements in non-coplanar directions at each temperature. If measurements in more directions are made (five in our case), a best tensor can be fitted and – in addition – the deviation of each experimental point from the best tensor can be evaluated, which is very useful for checking the consistency of the data. For the mathematical procedure of tensor evaluation the references [14,15] should be consulted. According to the definition of the material quantity *mobility* by the equation $v_i = \mu_{ij} E_j$, the coefficients i, j are a, b, c' in the orthogonalized crystallographic coordinate system, while $i = j = 1, 2, 3$ is used in the principal axes coordinate system, with the direction 1 as close to $+a$ as possible. Because the electron and the hole data obtained for the different samples had different lower bounds, probably due to accidentally introduced (structural) defects during sample preparation and handling, and because comparison of individual series of measurements with the best tensor data displayed larger deviations below certain temperatures, we limit the presentation of full tensor data to the temperature range from room temperature to 200K for holes and to 110K for electrons, where the estimated accuracy is better than ± 10% error deviation. The hole and the electron mobility tensor data in the orthogonalized crystallographic coordinate system are presented in the Tables II and III. Plots of the cross sections of the hole and of the electron tensor-ellipsoids in the *ac* plane of the crystal are shown in Fig. 8 and 9, respectively. The principal axes mobilities μ_{11} and μ_{33} are plotted in Fig. 10 and 11; for $\mu_{22} = \mu_{bb}$ see Fig. 4.

While, as a consequence of the monoclinic crystal symmetry, the direction of one tensor principal axis is fixed by symmetry constraints (in the common notation μ_{bb}), the orthogonal other two principal components can – at least in principle – rotate with temperature about b, as found before, see ref. [7] and Fig. 18 of ref. [4]. Such rotation is also found here, see Fig. 12; within the experimental error span the electron as well as the hole tensor clearly rotate in a continuous way (rotation angle α); the electron tensor with $m_\alpha^- = d\alpha^-(T)/dT = -0.035°/K$, with tendency to approach the a and c' crystallographic directions with its principal axes for $T \rightarrow 0K$, and with $\mu^-_{c'c'}$ the smallest mobility, as one might have conjectured intuitively from the π-electron overlap in the crystal structure [21]. The hole tensor, on the contrary, rotates fully unexpectedly, in the opposite sense, with $m_\alpha^+ = +0.06°/K$ into a ca. 45° orientation relative to a and c'. Notice that (1) in pure anthracene the mobilities of electrons and holes are rather similar (same order of magnitude)*, but (2) their anisotropies are qualitatively different; (3) the direction of fastest transport

* Over a wide temperature range (300 – 150 K).

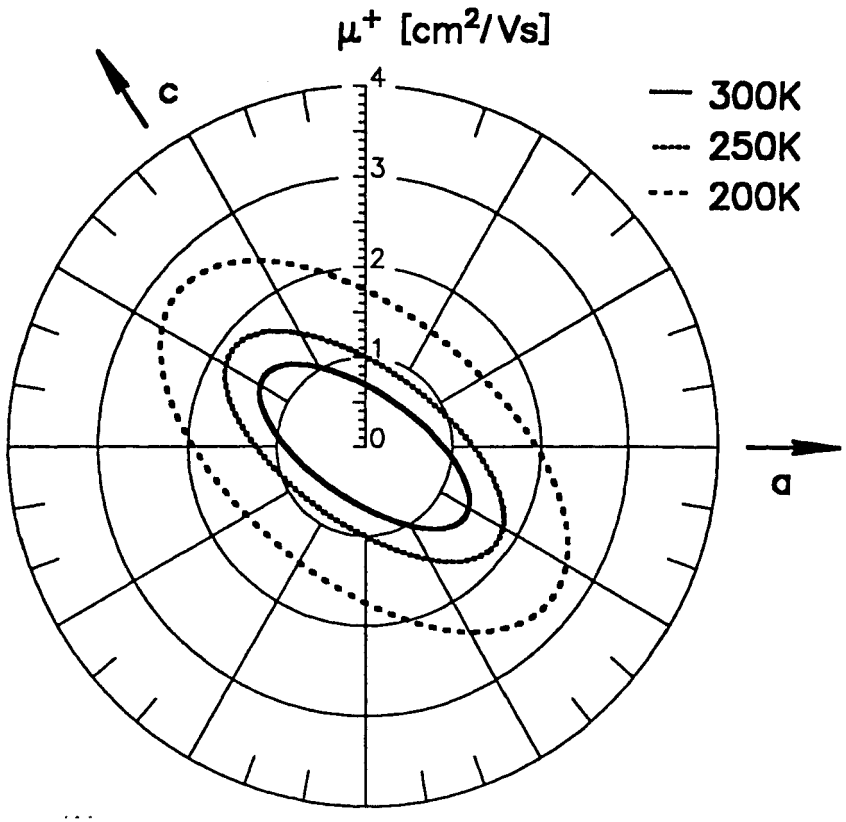

FIGURE 8 The hole mobility tensor ellipsoids in the *ac* plane for 300K, 250K, and 200K; the corresponding μ_{bb} values are 2.93, 3.74, and 5.05 cm^2/Vs, respectively, i.e. the fastest hole motion occurs along the crystallographic *b* direction

is for electrons along $\approx a$, whereas the holes exhibit the highest drift mobility in an orthogonal direction, along *b*, with an anisotropy $\mu_{11}:\mu_{22}:\mu_{33}$* reducing with decreasing temperature†. The anisotropic and sign-dependent magnitudes and temperature dependencies of the mobilities, as well as the cause of the tensor orientations and rotations are important signatures that a detailed adequate transport model – which is still lacking – would have to explain.

* Slightly.

† In contrast, the anisotropy of the electron mobility increases upon cooling; electron transport tends to become quasi-two-dimensional in the *ab*-plane, i.e. along the zig-zag-stacked molecular sheets.

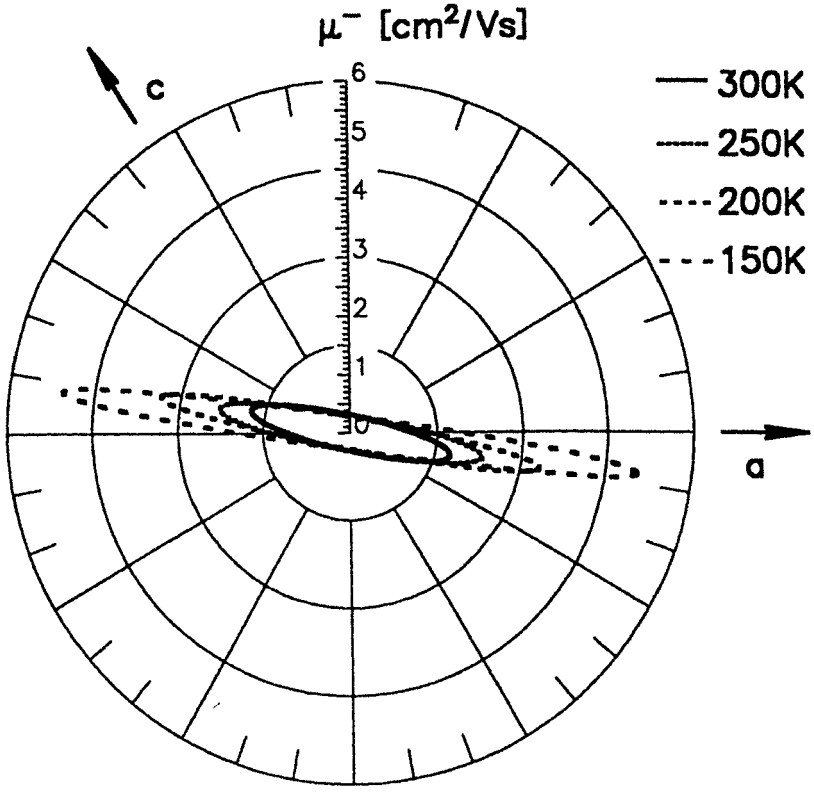

FIGURE 9 The electron mobility tensor ellipsoids in the *ac* plane for 300K, 250K, 200K, and 150K; the corresponding μ_{bb} values are 1.16, 1.39, 1.74, and 2.36 cm^2/Vs, respectively, i.e. the fastest direction for electron motion is near *a*

The mobility tensor component $\mu_{c'c'}$

The electron mobility in anthracene in c′ direction is surprisingly similar in both, the absolute values as well as the temperature dependence, to that in the next smaller homologue, naphthalene [5, 6; 7, 22; 17, 23]* which crystallizes in a similar crystal structure [24]. In both materials, upon cooling, a transition from a nearly temperature-independent electron mobility between above room temperature and 100K, to a continuously increasing one below is found at ca. 100K. As

* The minimum in the $\mu^-_{c'c'}$ curve reported in refs. [5,6] was absent in our purer samples [7,22]; in refs. [17,23] the principal axis mobility μ^-_{33} is plotted, which is close to $\mu^-_{c'c'}$ but may be considered to be more independent.

already mentioned, in the case of naphthalene this strange temperature dependence has been taken as a signature of a transition from a hopping type of transport at higher temperature to a band-type transport at lower temperatures [5,6]. Such transitions from one type of transport to another one had been theoretically predicted long ago [25], (see also more recent treatments of the problem [26–29], and the references given threrein, and a very recommendable, more general overview on electronic transport, ref. [30]).

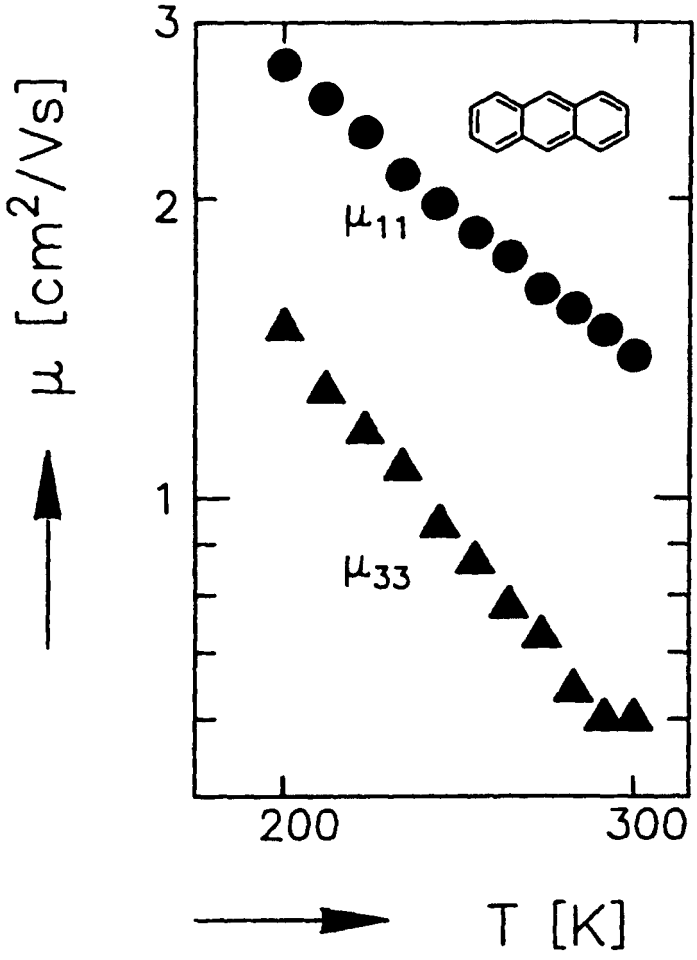

FIGURE 10 Principal hole mobilities in the ac plane, calculated from the experimental data, log μ versus log T plot. For the third principal mobility, $\mu_{bb}^{+} \equiv \mu_{22}^{+}$, see Fig. 4. The principal mobilities follow a temperature dependence $\mu_{11}^{+} \propto T^{-1.6}$, $\mu_{33}^{+} \propto T^{-2.3}$

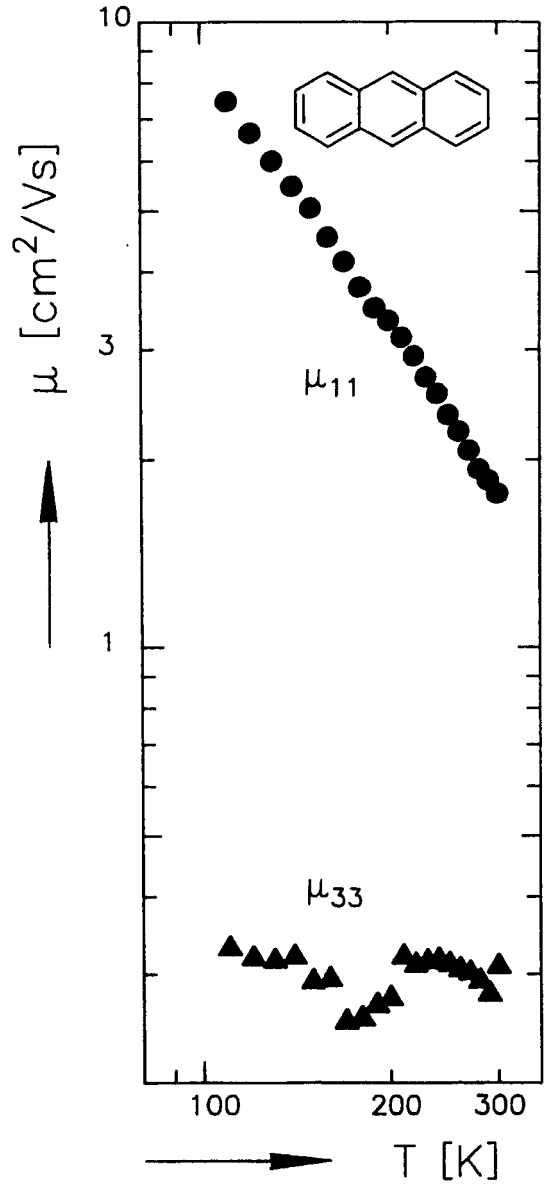

FIGURE 11 Principal electron mobilities in the ac plane, calculated from the experimental data, log μ versus log T plot. For the third principal mobility, $\mu_{bb}^{-} \equiv \mu_{22}^{-}$, see Fig. 4. The principal mobilities follow a temperature dependence $\mu_{11}^{-} \propto T^{-1.6}$, μ_{33}^{-}(in the temperature range plotted) approximately $\propto T^{-0.1}$

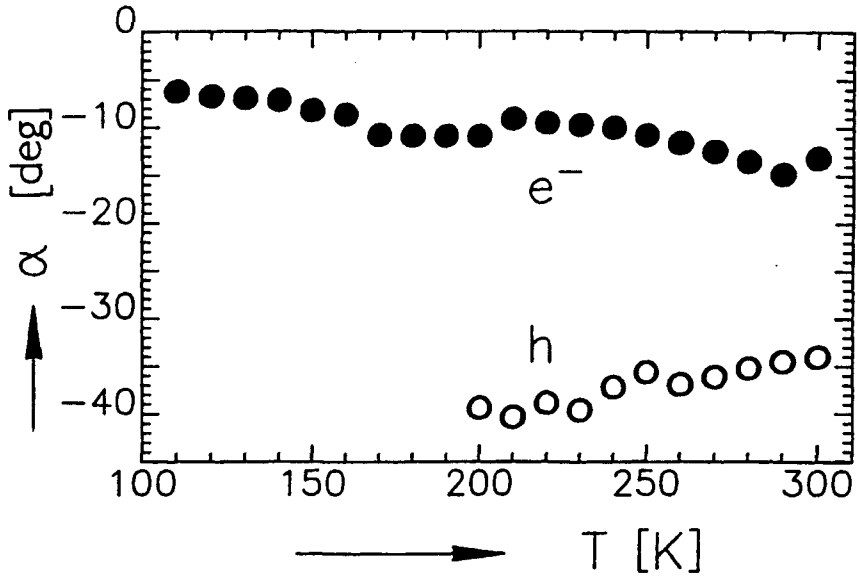

FIGURE 12 Rotation of the electron and of the hole mobility tensor about the crystallographic *b* axis with temperature. α is the angle between the crystallographic a axis and the largest mobility principal axis in the ac-plane, $\mu_{//}$, cf. caption of Fig. 2

In our view the experimetal results do not reflect an *abrupt* transition from one type of motion (incoherent hopping) to another type of motion (coherent band transport), as might have been conjectured from [5,6], but a rather independent superposition of both mechanisms, $\mu = \mu_{incoh} + \mu_{coh}$, with their relative weight changing with temperature, in accordance with the fundamental concepts of some of the proposed theoretical models [25–30]. A charge carrier in a given local environment (concerning density and correlations of the fluctuating intra- and intermolecular vibrational modes) has a certain probability P_{incoh} *or* P_{coh} per unit time to either proceed in its next motional step to a nearby molecule by (energetically) vertical – and therefore thermally activated – hopping, or by horizontal tunneling. These probabilities not only differ in their temperature dependencies, but are also different in different local environments and at different times, because of the fluctuations. As transport is based on a sequence of such events, the more probable process dominates the overall transport behavior.

Notice that this model does not assume a quasi-continuous microscopic motion at intermediate and higher temperatures but rather – at least for the coherent process – strongly fluctuating probabilities associated with the local fluctuations which stochastically open up paths of sufficient translational periodicity and equivalence

of levels across a certain (small) number of adjacent molecules, while there is always a certain (less fluctuating) "incoherent" transition probability for a charge carrier to hop across intermolecular atom – atom contacts. For the naphthalene crystal a deconvolution of the $\mu_{c'c'}$ mobility tensor component into a $\mu_{coh} \propto T^n$, $n < 0$, and a residual μ_{incoh} "hopping" part nicely demonstrates this sight of parallel channels (added probabilities): it turns out that the curve of the weakly temperature-dependent "hopping" part $\mu_{incoh,c}(T)$ contribution is surprisingly similar to that of the electron mobility in pyrene, the hole mobility in perylene, and the hole mobility in dipolarly disordered single crystalline 2,3-dimethylnaphthalene, cf. [23]. Obviously the "hopping motion" of charge carriers is not very substance-specific for condensed aromatic hydrocarbons, which, in retrospect, justifies the assumption that the very similar intermolecular atom – atom contacts are responsible for the hopping transfer. At the lower temperature range the coherent type of motion, in which the entire π-electron system is involved simultaneously, is faster, and hence the hopping part is concealed, while in the higher temperature range transport is dominated by the hopping contribution, and the coherent part is hidden. These results and ideas will be the subject of a separate paper.

Nonlinear transport

It has been checked independently by several authors for different pure organic crystals that a linear electric field – velocity relation holds for fields up to several kV/mm for mobilities ranging around a few cm^2/Vs, see e.g. [14, 31, 32]; for electrons drifting in c′ direction of anthracene linearity at 140K has even been confirmed up to 28kV/mm [33]. This is a manifestation of Ohms law. Eventually found nonlinearities could be traced back on either space charge perturbations of the applied field (i.e. false knowledge on the internal field), or on field assisted detrapping in impure crystals. It has therefore become mandatory to check the velocity – field relation to rule out perturbations which lead to wrong mobility data. An example of such a check is given in Fig. 13. At room temperature no deviation from Ohms law is seen for velocities up to several 10^4cm/s.

On the other hand, during such checks nonlinear transport has been discovered for organic photoconductors in the high mobility/high velocity – low temperature regime [8,9]. With the high quality anthracene samples available we were able to detect nonlinear transport also for this material for the fastest direction of the electrons, *a*, were transit pulses could still be obtained at temperatures well below 40K, see Fig. 14 [34]* . Similarly as for the electrons in *a* direction in naph-

* For thin (10μm) flakes of vapor-grown anthracene crystals fields as high as 100kV/mm could be applied. For E > 35kV/mm, corresponding to a *c′* hole velocity of $3 \cdot 10^5$cm/s marked sublinear deviations were observed already at room temperature [36].

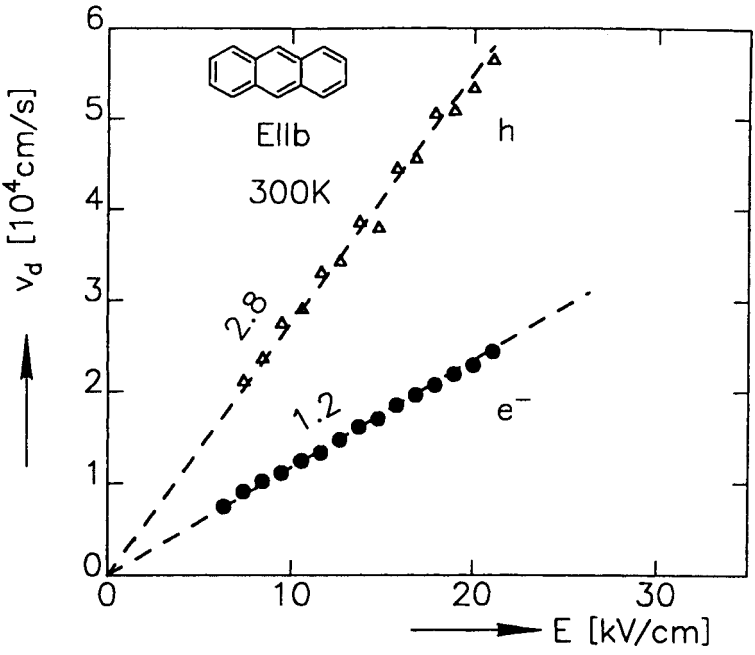

FIGURE 13 Check of the validity of Ohm's law, i.e. of a linear drift velocity – electric field relation at 300K in *b* direction. No deviations from linearity are seen up to a drift velocity of several 10^4 cm/s. The mobilities, corresponding to the slopes, are indicated (in units cm^2/Vs)

thalene [34], cf. [16], the electron velocity in the *a* direction of anthracene tends to *saturate* towards $(0.5 - 1)\cdot 10^6$cm/s at sufficiently low temperature (below 40K) and high fields ($2\cdot 10^4$V/cm). The saturation velocity is about a factor 5 higher than for the same direction and carrier sign in naphthalene. These results were already discussed in a previous paper [34]. Briefly, if the main cause of sublinear transport is assumed to be generative phonon scattering near the boundary of the Brillouin zone (generation of local, short wavelength phonons) and if the energy of the lowest optical phonon is taken representative for these inelastic processes, then from the transition from linear to field-saturated transport the energy of the hot electron (given off in the inelastic collision) can be estimated; together with its measured drift velocity this allows one to determine the effective mass of the electron. This idea has been elaborated in another previous paper [8].

Evaluation for the present case yields $m_{eff} = 15m_e$ at 36K and $m_{eff} = 5.4m_e$ at 20K [34]. These values compare surprisingly well with results of a cyclotron resonance experiment with holes orbiting in the *ab*-plane [35] (which, however, unfortunately, could not be reproduced). Thus, despite the smallness of the elec-

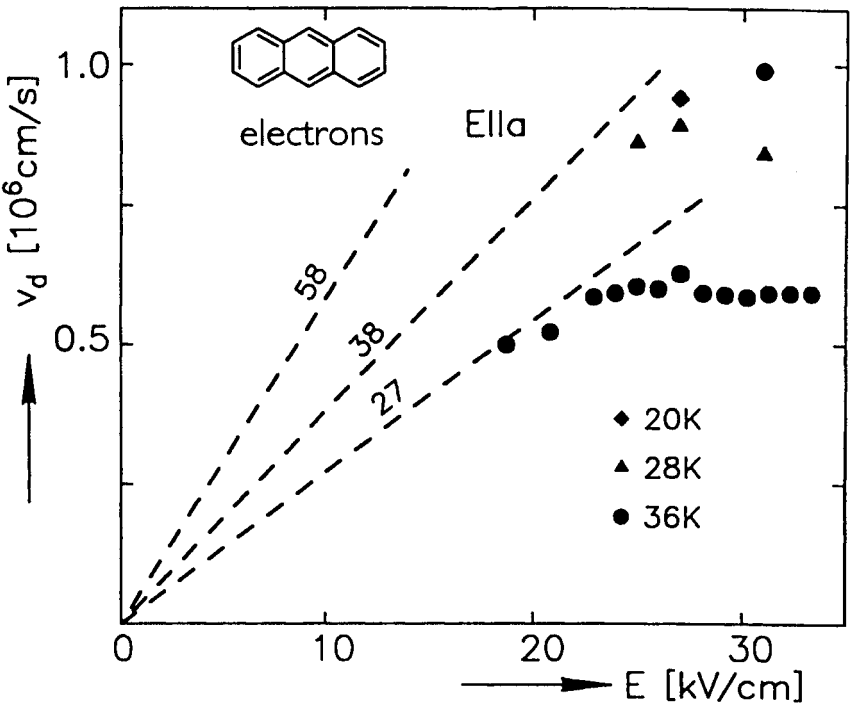

FIGURE 14 Check of the validity of Ohm's law for the electrons at 20K, 28K, and 36K in *a* direction. At these low temperatures the field dependence of the drift velocity is highly sublinear with a tendency to saturate around 10^6cm/s. The dashed lines visualize a reasonable range of lower field linear transport extrapolations (with the mobilities corresponding to the slopes, indicated in units cm^2/Vs); at the lower fields no TOF arrival time kinks could be observed anymore at these low temperatures (cf. Fig. 1b)

tronic interactions in this merely van der Waals bonded organic photoconductor, effective masses of charge carriers at low temperature can be rather small. For naphthalene, for which even 4K TOF data exist, it could be shown that m_{eff}/m_e of holes can approach a value close to 1 at the lowest temperatures [8, 34]. These results mean that at sufficiently low temperature where perturbing vibrations have essentially died out, electronic transport can proceed by comparatively fast coherent tunneling between the extended molecular π electron systems. As the charge carrier in this process is not localized to a substantial degree, the local interactions are short time and the slower response contributions to the additional polarization binding energy of the charge carrier, the phononic part and the vibronic part, can not come fully into play. Conversely, as temperature is raised, not only increased scattering rates decrease transport, but also, in turn, the decreased transport speed gives the charge carrier more time to polarize its sur-

rounding molecules and thus to become even more localized due to increased polarization interaction. Silinsh and coworkers have extended this view to assume an exponentially increasing effective mass with increasing temperature, see e.g. [26] and chapter 6.3.2 of ref. [37]. This mass can be interpreted in terms of a phonon energy and an electron – phonon coupling constant [38]. As soon as the mean free path between two scattering events which change the quantum state, approaches one molecular separation, the coherent band picture brakes down and some sort of incoherent transport model must take over. Nevertheless, occasional longer range coherent processes may still govern transport, albeit with a very small probability of occurrence, and hence with very small mobility.

There is certainly much room left for more sophisticated theoretical models which are detailed enough not to rely on one or two general parameters only, and which hopefully will finally be able to quantitatively reproduce the full anisotropic temperature dependent electron and the different hole mobility data, *and* the nonlinear transport behavior at low temperature/high velocity, for anthracene and for other related materials. The state of the art has been presented with great care in the book by Silinsh and Čápek [37].

Acknowledgements

This work was supported by the Fonds der Chemischen Industrie. We gratefully acknowledge the engagement and patience of Mr. Ch. Herb in purification and crystal growth of the material used.

References

1. R.G. Kepler, Phys. Rev. **119**, 1226 (1960).
2. O.H. LeBlanc, Jr. J. Chem. Phys. **33**, 626 (1960).
3. *anthracene mobility data published before 1984:*.
   R.G. Kepler in: Organic Semiconductors, (J.J. Brothy and J.W. Buttrey eds.), (The Macmilan Company, New York 1960), pp. 1 – 20.
   W. Helfrich and P. Mark Z. Physik **166**, 370 (1962).
   D.C. Hoesterey and G.M. Letson, J. Phys. Chem. Solids **24**, 1609 (1963).
   I. Nakada and Y. Ishihara, J. Phys. Soc. Japan **19**, 695 (1964).
   R. Raman and S.P. McGlynn, J. Chem. Phys. **40**, 515 (1964).
   C. Bogus, Z. Physik **184**, 219 (1965).
   C. Bogus, Z. Physik **207**, 281 (1967).
   T. Kajiwara, H. Inokuchi, and S. Minomura, Bull. Chem. Soc. Japan, **40**, 1055 (1967).
   T. Y. Maruyama and H. Inokuchi, Bull. Chem. Soc. Japan, **40**, 2073 (1967).
   K. Oyama and I. Nakada, J. Phys. Soc. Japan, **24**, 792 (1968).
   J. Fourny and G. Delacôte, J. Chem. Phys. **50**, 1028 (1969).
   G.T. Pott and D.F. Williams, J. Chem. Phys. **51**, 1901 (1969).
   N. Karl, E. Schmid und M. Seeger, Z. Naturforsch. 25a, 382- 391 (1970).
   R.W. Munn, J.R. Nicholson, W. Siebrand, and D.F. Williams, J. Chem. Phys. **52**, 6442 (1970).
   W. Mey, T.J. Sonnostine, D.L. Morel, and A.M. Hermann, J. Chem. Phys. **58**, 2542 (1973).
   K.H. Probst and N. Karl, Phys. Stat. Sol. a**27**, 499 (1975).
   R.G. Kepler, "Organic Molecular Crystals: Anthracene", review article in: Treatise in Solid State Chemistry **3**, (N.B. Hannay ed.), (Plenum Publ. Comp. New York 1976).

R.H. Young, W. Mey, and A.P. Marchetti, Appl. Phys. Lett. **30**, 38 (1977).
L.B. Schein, Chem. Phys. Lett. **48**, 571 (1977).
E.I.P. Walker, A.P. Marchetti, and R.H. Young, J. Chem. Phys. **68**, 4134 (1978).
L.B. Schein, R.W. Anderson, R.C. Enck, and A.R. McGhie, J. Chem. Phys. **71**, 3189 (1979).
L.B. Schein and A.R. McGhie, Chem. Phys. Lett. **62**, 356 (1979).
N. Karl, 9th Molecular Crystal Symposium (Mittelberg, Germany 1980), Conference Proceedings, pp. 149–152.
K. Yokoi, Japanese J. Appl. Phys. **19**, 2297 (1980).
L.B. Schein, R.S. Narang, R.W. Anderson, K.E. Meyer, and A.R. McGhie, Chem. Phys. Letters **100**, 37 (1983).

4. N. Karl, "Organic Semiconductors" in: Landolt-Boernstein (New Series), Group III, Vol. 17 Semiconductors (O. Madelung, M. Schulz, and H. Weiss eds.), Subvolume 17i, pp. 106–218 Springer-Verlag Berlin, Heidelberg, New York, Tokyo 1985.
5. L.B. Schein, C.B. Duke, and A.R. McGhie, Phys. Rev. Lett. **40**, 197 (1978).
6. L.B. Schein and A.R. McGhie, Phys. Rev. B **20** 1631 (1979).
7. N. Karl, 9th Molecular Crystal Symposium (Mittelberg, Germany 1980), Conference Proceedings, pp. 149–152.
8. W. Warta and N. Karl, "Hot Holes in Naphthalene: High, Electric Field-Dependent Mobilities", Phys. Rev. B32, 1172–1182 (1985).
9. W. Warta, R. Stehle, and N. Karl, Appl. Phys. A36, 163–170 (1985).
10. N. Karl and J. Marktanner, 1991, unpublished.
11. N. Karl, Dissertation (PhD thesis), University of Freiburg/Brg. (1968).
12. N. Karl, E. Schmid and M. Seeger, Z. Naturforsch. 25a, 382–391 (1970).
13. W. Warta, R. Stehle, and N. Karl, Appl. Phys. A36, 163–170 (1985).
14. D. Massa and N. Karl, Mol. Cryst. Liq. Cryst. 175, 93–117 (1989).
15. D. Massa, Dissertation (PhD thesis), Universität Stuttgart (1988).
16. N. Karl, "Getting beyond Impurity-limited Transport in Organic Photoconductors" in: Defect Control in Semiconductors, Vol. II, (K. Sumino, ed.) pp. 1725–1746 (North Holland, Amsterdam 1990).
17. N. Karl "Kurzzeitspektroskopische Untersuchungen zum Ladungstraegertransport in einkristallinen (organischen) Photoleitern" in: Spektroskopie amorpher und kristalliner Festkoerper (D. Haarer and H.W. Spiess (eds.): Steinkopff Verlag (Darmstadt 1995), pp. 453–481.
18. H. Scher and E.W. Montroll, Phys. Rev. B **12**, 2455 (1975).
19. N. Karl "High Purity Organic Molecular Crystals" in.: Crystals, Growth, Properties and Applications (H.C. Freyhardt, ed.) (Springer Verlag, Berlin 1980), pp 1 –100.
20. N. Karl, H. Port, and W. Schrof, Mol. Cryst. Liq. Cryst. **78**, 55 (1981).
21. A. McL. Mathieson, J.M. Robertson, and V.C. Sinclair, Acta Cryst. **3**, 245 (1950).
22. N. Karl, Materials Science (Univ. of Wroclaw, Poland) **10**(3), 365 (1984).
23. N. Karl, 11th Molecular Crystal Symposium, Lugano (Switzerland) 1985, Conference Proceedings, pp. 137 – 142.
24. P.C. Brock and J.D. Dunitz, Acta Cryst. B **38**, 2218 (1982).
25. T. Holstein, Ann. Phys. (N.Y.) **8**, 325 and 343 (1959).
26. E.A. Silinsh, A. Klimkāns, S. Larsson and V. Čápek. Chem. Phys., 198, 311 (1995).
27. R. Silbey and R.W. Munn, J. Chem. Phys. **72**, 2763 (1980).
28. R.W. Munn, Inst. Phys. Conf. Ser. **58**, 98 (1981).
29. V. Čápek and R.W. Munn, Phys. Stat. Sol. (b) **108**, 521 (1981) and **109**, 245 (1982).
30. G.G. Robertson, N. Aspley, and R.W. Munn, Physics Reports **60**, 59–150 (1980).
31. G.A. Cox and P.C. Knight, J. Phys. C: Solid State Phys. **7**, 146 (1974).
32. Z. Burshtein and D.F. Williams, Phys. Rev. B **15**, 5769 (1977).
33. L.B. Schein, R.S. Narang, R.W. Anderson, K.E. Meyer, and A.R. McGhie, Chem. Phys. Letters **100**, 37 (1983).
34. N. Karl, J. Marktanner, R. Stehle, and W. Warta Synthetic Metals 42/3, 2473–2481 (1991).
35. D.M. Burland, Phys. Rev. Lett. **33**, 833 (1974); D.M. Burland and U. Konzelmann, J. Chem. Phys. **67**, 319 (1977).
36. K. Bitterling and F. Willig, Phys. Rev. B **35**, 7973 (1987).
37. E.A. Silinsh and V. Čápek, "Organic Molecular Crystals", (American Inst. of Phys., New York 1994).

38. C.E. Swenberg and M. Pope, Chem. Phys. Letters **287**, 535 (1998).
39. Comparison of that part of the present results, which was obtained in the upper temperature regime, with earlier ones: At 300K the μ_{aa}^{+}, μ_{aa}^{-} and $\mu_{c'c'}^{-}$data agree with our earlier results (see [7] [7,40] and the data compilation of ref. [4]) within better than 3%; μ_{bb}^{-}: μ_{bb}^{-} had been found 9%, $\mu_{c'c'}^{+}$ 14% smaller before, and, most strikingly, μ_{bb}^{+}even 29% smaller, although for the latter the temperature exponent n_b^{+} agrees within 5%; as the present μ_{bb}^{-}, measured with the same sample is 9% larger, part of the μ_{bb}^{+} increase probably reflects higher crystal quality of [16] while the other part could be due to a thickness error ΔL which enters the μ error twice ($\Delta\mu/\mu = 2\Delta L/L$); notice that a μ_{bb} error would, however, not influence the other tensor components. The fact that $\mu_{c'c'}^{+}$ and $n_{c'}^{+}$ are both substantially larger than found before is thought to also reflect the higher quality of the sample available in the present investigation, which is also supported by the fact that the nearly temperature-independent electron mobility component $\mu_{c'c'}^{-}$could be followed further down (to 40K) for this sample and there found to display an increase – for the first time. The stronger temperature dependence of $\mu_{c'c'}^{+}$ leads to a small temperature rotation also of the hole tensor, while the rotation of the electron tensor, m_{α}^{-} is confirmed quantitatively, albeit with a small, temperature-independent offset of the orientation of the principal axis system by −11° (-7° for the hole tensor at 300K) relative to the earlier results. The exponents n_a^{+}, n_b^{+}, and $n_{c'}^{-}$ agree with the earlier results within the experimental error span; n_a^{-} was reported 15% larger, n_b^{-} 14% smaller before, Thus, in view of the better crystal quality and of the experimental error bars, the new data are in fair consistence with the earlier data concerning the overlapping temperature range.
40. W. Warta, Diplomarbeit, University of Stuttgart 1978.